American Journal of Pathology, Vol. 143, No. 4, October 1993

Technical Advances

Dorsal Skinfold Chamber Technique for Intravital Microscopy in Nude Mice

Hans-Anton Lehr, Michael Leunig, Michael D. Menger, Dirk Nolte, and Konrad Messmer

From the Institute for Surgical Research, Klinikum Grosshadern, University of Munich, Munich, Germany

For many years, observation chambers, implanted in various animal species and in man, have been used for intravital microscopy of the microcirculation in granulation tissue, preformed tissue, or of the microvascularization of tissue implants. We describe herein a skinfold chamber model for the intravital microscopic investigation of striated skin muscle in immunoincompetent, nude mice over a minimum period of 2 weeks. Using fluorescent markers for contrast enhancement of plasma (fluorescein isothiocyanate–dextran) and leukocytes (acridine orange), the presented model allows the quantitative analysis of 1) the microhemodynamic parameters microvessel diameter and red blood cell velocity in arterioles (16 to 50 μ diameter), capillaries (4 to 9 μ diameter), and postcapillary venules (19 to 60 μ diameter), 2) leukocyte/endothelium interaction in these vessel segments, 3) functional capillary density and intercapillary distance, and 4) endothelial cell integrity. These parameters can be assessed in the microcirculation of the striated muscle tissue under normal or pathological conditions, as well as in the microcirculation of transplanted xenogeneic (human) neoplastic and non-neoplastic tissue grafts. (Am J Pathol 1993, 143:1055–1062)

In 1924, Sandison[1] was the first to implant observation chambers into animals for intravital microscopy of living tissues. Since then, various chambers have been developed and implanted with the aim to investigate the microcirculation in mice,[2] hamsters,[3] rats,[4] rabbits,[5,6] and even in human subjects.[7] The tissue under microscopic observation was either preformed tissue, mostly striated skin muscle and subcutaneous tissue[8–10] or newly formed granulation tissue.[2,4,6,11] To facilitate the access to the chamber and to allow the microscopic investigation in restrained but unanesthetized animals, chambers were implanted into the dorsal skinfold in mice,[8] rats,[10] and hamsters.[9] These models have been applied to the study of the autochtonous microvasculature, but also of the growth and microvascularization of transplanted neoplastic[10,12] and nonneoplastic tissue.[13–15]

Because the microvasculature constitutes the principal requisite for the growth of neoplastic tissue,[12] many chamber model approaches have addressed the susceptibility of the tumor microvasculature to therapeutic interventions, including hyperthermia and shock wave therapy.[16,17] The advent of antitumor therapies involving tissue-specific monoclonal antibodies,[18] lymphokine-activated killer cells,[19] antisense oligonucleotides,[20] and single gene products[21] has now created the need for models allowing the direct investigation of the microcirculation in human neoplastic xenografts. Nude animals, deficient in cell-mediated immunity due to recessive thymic aplasia, have been used frequently in the last years as hosts for the transfer of human xenogeneic malignant tumors.[22] These transplanted tumors have been shown to retain their original histological and chromosomal pattern as well as their antigenic, enzymatic, and functional characteristics.[22]

To allow for intravital fluorescence microscopy of the microcirculation of transplanted xenogeneic human-derived tumors in immunoincompetent ani-

Accepted for publication June 3, 1993.

Address reprint requests to Dr. Hans-Anton Lehr, Dept. of Pathology, University of Washington, RC-72, 1959 NE Pacific St., Seattle, WA 98195.

mals, we have adapted the hamster dorsal skinfold chamber model to the use in nude mice. In this study, we demonstrate the assembly and implantation of specifically manufactured titanium chambers, the methods of intravital fluorescence microscopy, and the microvascular characteristics of the striated muscle microcirculation later to serve as the host vasculature for the growth of transplanted human tissue grafts.

Materials and Methods

Animal Model

Dorsal skinfold chambers and indwelling venous catheters were implanted in 11- to 13-week-old nude mice (26 to 33 g body weight; Crl:nu/nu; Charles River, Inc., Sulzfeld, Germany), anesthetized by subcutaneous injections of 0.1 ml of a saline solution containing 3.75 mg ketamine hydrochloride (Ketavet, Parke Davis, Freiburg, Germany) and 0.5 mg dihydroxylidinothiazin hydrochloride (Rompun, Bayer, Leverkusen, Germany). The animals were bred and maintained in a pathogen-free environment with free access to laboratory chow and sterilized water.[23]

Surgical Technique

The titanium frames (total weight 3.2 g) used for implantation in the dorsal skinfold of nude mice were manufactured analogously—however, smaller in size—to those previously made from aluminum[9] and titanium[24] for dorsal skinfold chamber preparations in hamsters.[9] Titanium was chosen to increase stability of the frames, to guarantee biological inertness, and to reduce thermal conductivity. This is a crucial advantage over aluminum chamber frames used earlier in the hamsters model[9] and in previously presented chamber models.[10] The microsurgical technique used for the implantation of chambers and indwelling venous catheters was similar to that described previously for Syrian golden hamsters.[9,24] The frames were implanted so as to sandwich the extended double layer of skin, perpendicular to the animal's back (Figure 1). Using an operation microscope and microsurgical instruments, one layer of skin was completely removed in a circular area of 15 mm in diameter, and the remaining layer, consisting of epidermis, subcutaneous tissue, and a thin striated skin muscle, was covered with a coverslip incorporated in one of the frames. Using stainless steel nuts as spacers, a frame-to-frame distance of 400 to 450 μ was chosen to prevent compression of nutritional blood vessels.

Fine polyethylene catheters (PE 10, inner diameter 0.28 mm) were inserted into the jugular vein and the carotid artery, respectively, passed subcutane-ously to the dorsal side of the neck, closed, and sutured to the titanium frames (Figure 1). The animals tolerated the chambers and indwelling catheters well and showed no signs of discomfort. In particular, no effect on sleeping and feeding habits were observed.

Intravital Fluorescence Microscopy

After chamber implantation, the animals were kept in separate cages with free access to laboratory chow and sterilized water. A recovery period of 72 hours between implantation of the skinfold chamber and the microscopic investigation was allowed to eliminate the effects of anesthesia and immediate surgical trauma on the chamber tissue. For intravital microscopy, the mice were positioned in a plexiglass tube of approximately the same diameter as the animal in a crouched position. A narrow longitudinal slot allowed only the observation window of the chamber to stick out of the tube. The tube was then fixed on a plexiglass platform, which was placed on the microscope stage. For contrast enhancement of the intravascular space, 0.2 ml of fluorescein isothiocyanate-labeled dextran (FITC-dextran M_r150 k, 5 mg/100 μl of physiological saline solution; Sigma Chemical Co., Deisenhofen, Germany) was infused intravenously into the animals. Leukocytes were visualized by intravenous infusion of the fluorescent marker acridine orange (0.5 mg/kg/minute; Sigma). Epiillumination was achieved with a 75 W, DC, xenon lamp attached to a Ploemopak illuminator (Leitz Inc., Wetzlar, Germany) with an I_2 filter block. The microscopic images (25-fold water immersion objective from Leitz Inc., total magnification 560-fold; Camera COHU FK6990; Prospective Measurements,

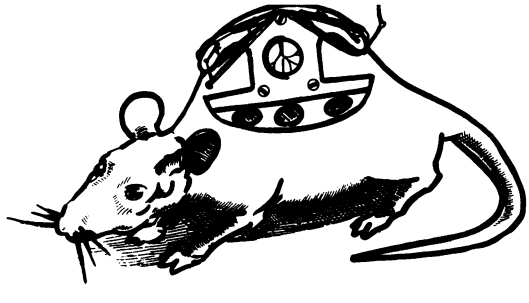

Figure 1. *Nude mouse with dorsal skinfold chamber.*

San Diego, CA) were recorded on video tape at a rate of 50 frames per second. Microvessel diameter and red blood cell (RBC) velocity were analyzed off-line using a computer-assisted image analysis system (CapiFlow, IM-CapiFlow, Stockholm, Sweden). Functional capillary density (FCD) was defined as the total length of capillaries with red cell flow (plasma contrast enhanced with FITC-dextran M_r 150 k) as opposed to unperfused capillaries per observation area (Figure 2B). FCD was analyzed using a computer-assisted microcirculation analysis system[13,32] and is given in cm/cm^2. The average distance between capillaries (μ) was assessed by CapiFlow. The obtained data are depicted in Table 1 and compared to respective data obtained in a similar skinfold chamber model in hamster.[9]

Results

Implantation of Skinfold Chambers

The implantation of the ultralight titanium frames as well as the intravital microscopic examinations were well tolerated by the nude mice. The chambers were examined under a photomacroscope 3 days after implantation. Impaired microvascular blood flow and signs of inflammation (hyperemia, distortion of venular segments, edema formation, adhesion of circulating leukocytes to the venular endothelium[9]) resulted in the exclusion of the chambers from the experiments. Despite the deficient immune system in nude mice, we observed no higher incidence of inflammatory complications due to either mechanical trauma or bacterial contamination

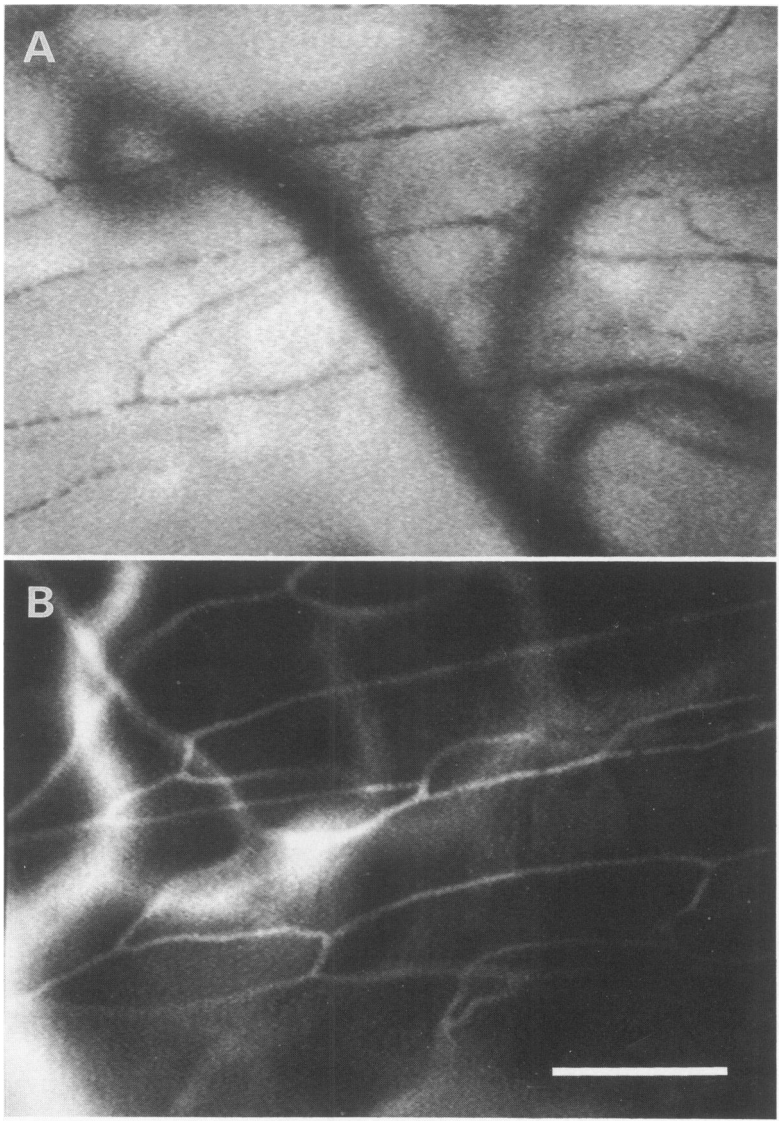

Figure 2. *Capillary network in striated muscle. Capillaries of the striated muscle, discerned either by visualization of RBCs (443-nm narrow band filter transillumination* [A]*) or by epiillumination using FITC-dextran as intravascular marker (I_2 blue filter block; λ_{ex}450 to 490 nm λ_{em} >510 nm* [B]*). Scale bar represents 100 μ.*

Table 1. *Macro- and Microhemodynamic Parameters in Nude Mice as Compared to Hamsters*

	Nude mice	Hamsters
Species		
MAP (mm Hg)	87 ± 11 (n = 8)	93 ± 9 (n = 8)
HR (1/min)	446 ± 66 (n = 8)	353 ± 30 (n = 8)
FCD (cm/cm^2)	249 ± 12 (n = 30) (range: 180–312)	184 ± 18 (n = 42) (range: 110–244)
ICD (μ)	37 ± 15 (n = 40) (range: 11–72)	54 ± 28 (n = 40) (range: 20–84)
Diameters (μm)		
Arterioles	37.4 ± 12.8 (n = 18) (range: 16–50)	42.2 ± 14.1 (n = 30) (range: 17–52)
Capillaries	5.6 ± 1.8 (n = 19) (range: 4–9)	6.1 ± 1.4 (n = 30) (range: 5–10)
Venules	41.5 ± 10.6 (n = 45) (range: 19–60)	46.5 ± 13.0 (n = 30) (range: 19–65)
RBC velocities (mm/sec)		
Arterioles	> 2	> 2
Capillaries	0.12 ± 0.03 (n = 19) (range: 0.08–0.26)	0.13 ± 0.04 (n = 30) (range: 0.1–0.28)
Venules	0.78 ± 0.13 (n = 45) (range: 0.50–1.7)	0.72 ± 0.20 (n = 30) (range: 0.5–1.6)

MAP = mean arterial pressure; HR = heart rate; ICD = intercapillary distance. FCDs were assessed by computer-assisted microcirculation analysis system.[13,26] Vessel diameters and RBC velocities were assessed by CapiFlow. Data are given as mean ± SD and the range. Data for the hamster are taken from refs. 9 (mean arterial pressure, heart rate), 32 (FCD), and 24 (intercapillary distance, diameter, RBC velocity).

(approximately 1 to 2 out of 10 implanted chambers) when compared to hamsters[27] and hairless mice.[28]

Intravital Fluorescence Microscopy

Intravital microscopy was first performed on day 3 after implantation of skinfold chambers. Reevaluation was performed on days 3, 7, and 14 after the initial observation. Videomicroscopy yielded high quality imaging of the microvascular bed at various focus levels, visualizing either the capillary network of striated muscle (straight, parallel capillaries; Figures 2; 4B) or the larger precapillary or postcapillary vessel segments in the subcutaneous tissue immediately adjacent to the striated muscle (Figures 3 and 4A). Over the entire time period of the microscopic observation, the macromolecular marker FITC-dextran was retained within the intravascular space (Figures 2B and 3), and indicating that the endothelial integrity was preserved.[29] In some animals, image quality was slightly reduced at later observation time points due to repeated infusions of

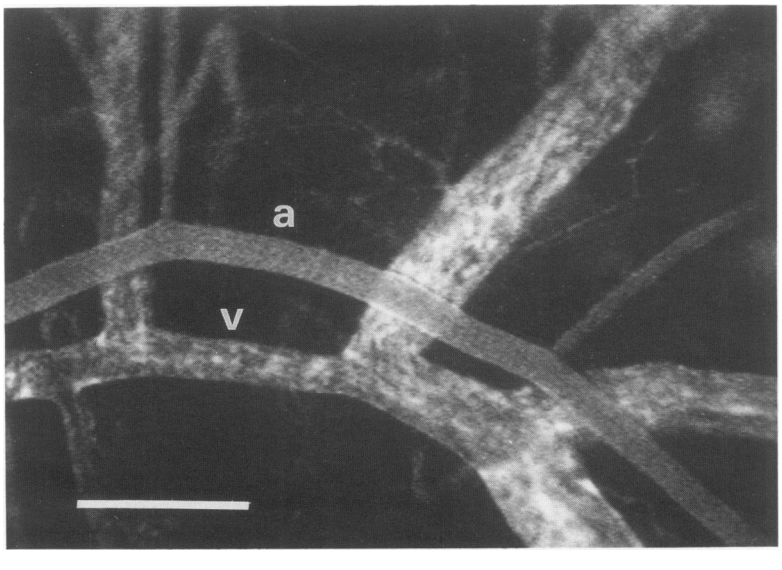

Figure 3. *Visualization of arterioles and venules in the subcutaneous tissue adjacent to the striated muscle. Arteriole (a) and collecting venule (v). Scale bar represents 100 μ.*

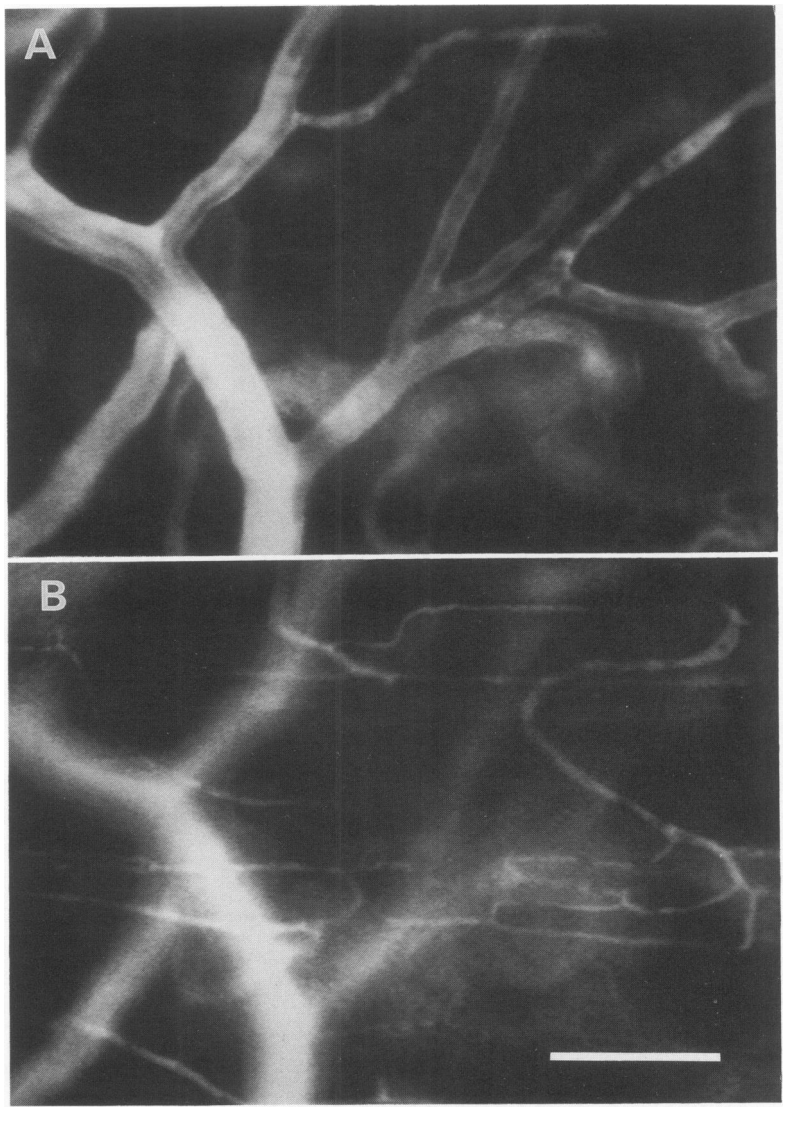

Figure 4. *Microvascular segments in adjacent focus levels. Postcapillary/collecting venules in the tissue layer adjacent to the striated muscle* (A) *and capillary network* (B) *within the striated muscle as assessed by intravital fluorescence microscopy using FITC-dextran as intravascular marker. Note the differences in microvascular hematocrit as reflected by differences in fluorescence intensity of FITC-dextran. Scale bar represents 100 μ.*

the fluorescent marker, resulting in higher levels of background fluorescence. However, image quality was always sufficient for qualitative and quantitative analysis of the microcirculatory parameters. The microcirculatory data assessed in the animals in this study are depicted in Table 1. All values obtained in the 2-week follow-up period (days 3, 7, and 14 after initial observation) remained within a 10% range of the baseline measurements. We did not observe pathologically enhanced leukocyte/endothelium interaction in postcapillary or collecting venules at day 3 or at later observation time points, nor did we observe adhesive leukocytes in arterioles or leukocytes plugging the lumen of capillaries. In postcapillary and collecting venules, the number of sporadic sticking leukocytes never exceeded one cell per 200 μ vessel segment at any time point. However, a steady fraction of leukocytes (approximately 25% of all leukocytes) rolled along the endothelial lining in venules at a considerably lower velocity when compared to the erythrocyte velocity. However, in agreement with earlier findings in the hamster model,[24] leukocyte rolling and sticking was dramatically increased by exposure of the muscle tissue to a temporal, pressure-induced ischemia, followed by 30 minutes of reperfusion (Figure 5, A and B).

In addition to studies on the microcirculation of striated muscle under normal and pathophysiological conditions, the skinfold chamber model allows the study of the revascularization of syngeneic and xenogeneic (human) neoplastic and non-neoplastic tissue grafts (Figure 6).

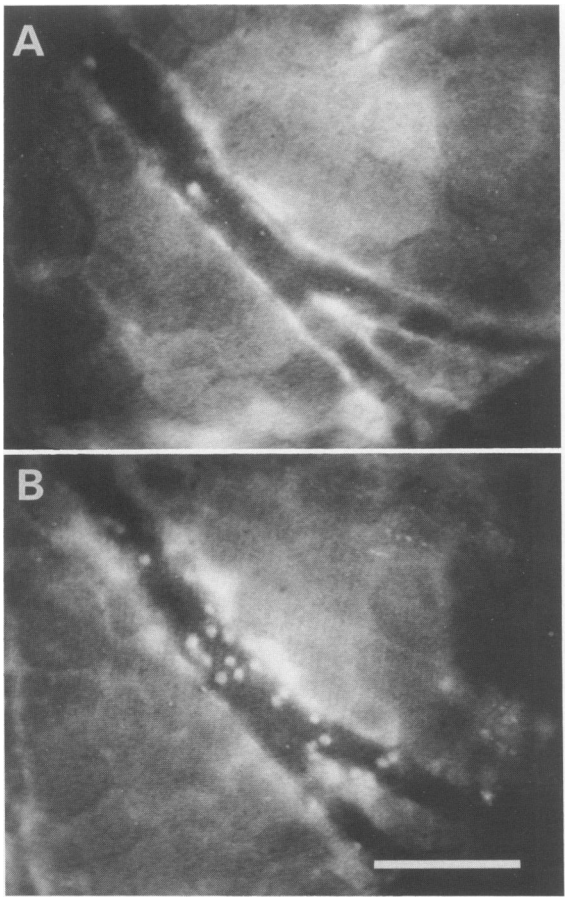

Figure 5. *Leukocyte/endothelium interaction in venules. Leukocyte/endothelium interaction was assessed before* (**A**) *and after a 4-hour ischemia of the muscle tissue followed by 30 minutes of reperfusion* (**B**). *Leukocytes are stained in vivo with acridine orange. Scale bar represents 100 μ.*

Discussion

Skinfold Chamber Model

The presented model allows the intravital microscopy of preformed striated muscle tissue in the dorsal skinfold of nude mice. The significance of experiments in biological models is based on intact physiological conditions of the object under observation. For the purpose of intravital microscopy of the microcirculation, the physiological properties of the studied tissue have to be thoroughly scrutinized. Inflammatory complications due to either mechanical trauma or bacterial contamination, heralded microscopically by hyperemia, distortion of venular segments, edema formation, and the adhesion of circulating leukocytes to the venular endothelium,[9] lead to the exclusion of the animals from the experiments. In this respect, the presented model exhibits marked advantages over previously used chamber models: physiological conditions are not provided in newly formed tissue, grown in granulation tissue chambers in response to stimuli of wound healing or inflammation.[2,4,6,11]

In the time course of the experiments, we observed a slight loss of contrast quality in the chamber tissue. However, the absence of signs of inflammation, in particular, leukocyte adhesion to the venular endothelium[30] and alterations in capillary perfusion, suggest that these changes may be ascribed to the repeated injections and reabsorption of FITC-dextran.

To further reduce the influence of artifacts in our model, animals were allowed a 72-hour period to recover from anesthesia and the direct surgical trauma associated with chamber implantation. Finally, it should be noted that all intravital microscopic examinations can be performed on awake, unanesthetized animals to exclude effects of anesthetic drugs on the microcirculation.[31]

Microcirculatory Findings

The microhemodynamic data assessed in the nude mice in this study correspond well with observations in a similar skinfold chamber model in hamsters[9,24,32] (Table 1) and in various other microcirculatory models (reviewed in ref. 9). The markedly higher functional capillary density and the reduced intercapillary distance in striated muscle in nude mice when compared to hamsters (Table 1) reflects an adaptation of the microvasculature to the higher metabolic rate and oxygen consumption in the muscle tissue in these animals.[33] Anatomically, the skin muscle in nude mice consists of two or more layers of muscle fibers with a dense interconnecting capillary network, whereas in the hamster it is formed of only one layer of muscle.[9]

In addition to the microhemodynamic parameters described in this study under physiological conditions, the model allows the investigation of morphological and functional changes of the microcirculation as induced by various stimuli such as ischemia/reperfusion injury or systemic and local administration of chemotactic agents.[24,28] The parameters under investigation include the extravasation of fluorescently labeled macromolecules across a damaged endothelium,[29] changes in functional capillary density, (Figures 2 and 4B) or the interaction of fluorescently labeled leukocytes with the microvascular endothelium (Figure 5, A and B).

Potential Applications of the Model

Previous studies on the dorsal skinfold chamber model in the hamster imply that the presented nude

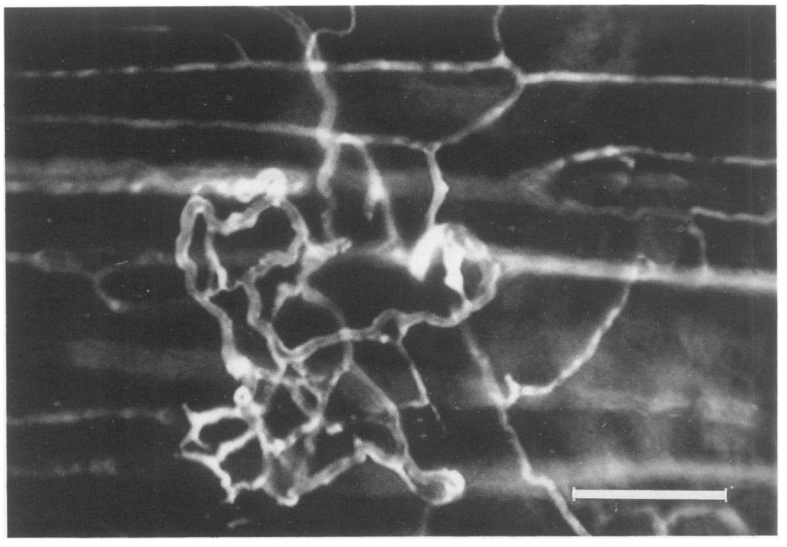

Figure 6. *Microvasculature of a syngeneic pancreatic islet graft 10 days after transplantation into the dorsal skinfold chamber. Scale bar represents 100 μ.*

mouse model may be used to study the microcirculatory response to ischemia/reperfusion injury[24,32] or the response to either local or systemic administration of inflammatory mediators,[24] toxins, drugs, or other stimuli.[16,28] The transfer of the skinfold chamber model to the mouse allows monoclonal antibodies to be utilized, for instance, those directed against adhesion molecules for leukocyte/endothelium interaction that are not available for the hamster to date. In addition, the adaptation of the skinfold chamber model to an immunoincompetent animal species offers unique possibilities for the investigation of problems related to the transfer of xenogeneic (ie, human) neoplastic[23,34] or non-neoplastic material, eg, the transplantation of human islets of Langerhans into nude mice, in analogy to a previously established syngeneic procedure in hamsters[15] (Figure 6).

References

1. Sandison JC: The transparent chamber of the rabbit's ear giving a complete description of improved techniques of construction and introduction and general account of growth and behavior of living cells and tissues as seen with the microscope. Am J Anat 1928, 41:447–472
2. Algire GH: An adaptation of the transparent chamber technique to the mouse. J Natl Cancer Inst 1943, 4:1–11
3. Greenblatt M, Shubik P: Hamster cheek pouch chamber. Cancer Bull 1967, 19:65–81
4. Hobbs JB, Chusilp S, Hua A, Kincaid-Smith P, McIver MA: The pathogenesis of hypertensive vascular changes in the rat: microscopic and ultrastructural correlation in vivo. Clin Sci 1976, 51:71s–75s
5. Arfors KE, Jonsson JA, McKenzie FN: A titanium rabbit ear chamber: assembly, insertion, and results. Microvasc Res 1970, 2:516–519
6. Clark ER, Kirby-Smith HT, Rex RO, Williams RG: Recent modifications in the method of studying living cells and tissues in transparent chambers inserted in the rabbit's ear. Anat Rec 1930, 47:187–211
7. Brånemark PL, Aspegren K, Breine U: Microcirculatory studies in man by high resolution vital microscopy. Angiology 1964, 15:329–332
8. Cardon SZ, Ostermeyer CF, Bloch EH: Effect of oxygen on red blood cell flow in unanesthetized mammalian striated muscle as determined by microscopy. Microvasc Res 1970, 2:67–76
9. Endrich B, Asaishi K, Goetz A, Messmer K: Technical report—a new chamber technique for microvascular studies in unanesthetized hamsters. Res Exp Med 1980, 177:125–134
10. Papenfuss HD, Gross JF, Intaglietta M, Treese FA: A transparent access chamber for the rat dorsal skin fold. Microvasc Res 1979, 18:311–318
11. Falkvoll KH, Rofstad EK, Brustad T, Marton P: A transparent chamber for the dorsal skin fold of athymic mice. Exp Cell Biol 1984, 52:260–268
12. Oda T, Lehmann A, Endrich B: Capillary blood flow in the amelonotic melanoma of the hamster after isovolemic hemodilution. Biorheology 1984, 21:509–520
13. Messmer K, Funk W, Endrich B, Zeintl H: The perspectives of new methods in microcirculation research. Prog Appl Microcirc 1984, 6:77–90
14. Funk W, Endrich B, Messmer K: A novel method for follow-up studies of the microcirculation in nonmalignant tissue implants. Res Exp Med 1986, 186: 259–270
15. Menger MD, Jäger S, Walter P, Hammersen F, Messmer K: A novel technique for studies on the microvasculature of transplanted islets of Langerhans in vivo. Int J Microcirc Clin Exp 1990, 9:109–117

16. Brendel W, Goetz A, Delius M: Effect of shock waves on the microvasculature. Prog Appl Microcirc 1987, 12:41–50
17. Endrich B, Hammersen F, Messmer K: Hyperthermia-induced changes in tumor microcirculation. Recent Results Cancer Res 1988, 107:44–59
18. Dillman RO: Monoclonal antibodies for treating cancer. Ann Intern Med 1989, 111:592–603
19. Sacchi M, Vitolo D, Sedlmayr P, Rabinowich H, Johnson JT, Herberman RB, Whitesied TL: Induction of tumor regression in experimental model of head and neck cancer by human A-LAK cells and IL-2. Int J Cancer 1991, 47:784–791
20. Zamecnik PC, Stephenson ML: Inhibition of Rous sarcoma virus replication and cell transformation by a specific oligonucleotide. Proc Natl Acad Sci USA 1978, 75:280–284
21. Dumenco LL, Arce C, Norton K, Yun J, Wagner T, Gerson SL: Enhanced repair of O^6-methylguanine DNA adducts in the liver of transgenic mice expressing the ada gene. Cancer Res 1991, 51:3391–3398
22. Giovanella BC, Fogh J: Present and future trends in investigations with the nude mouse as a recipient of human tumor transplants. The Nude Mouse in Experimental and Clinical Research. Edited by Fogh J, Giovanella BC. New York, Academic Press, 1978, pp 282–312
23. Giovanella BC, Stehlin JS: Heterotransplantation of human malignant tumors in "nude" thymusless mice. I. Breeding and maintenance of "nude" mice. J Natl Cancer Inst 1973, 51:615–619
24. Lehr HA, Guhlmann A, Nolte D, Keppler D, Messmer K: Leukotrienes as mediators in ischemia-reperfusion injury in a microcirculation model in the hamster. J Clin Invest 1991, 87:2036–2041
25. Lehr HA, Hübner C, Nolte D, Kohlschüter A, Messmer K: Dietary fish oil blocks the microcirculatory manifestations of ischemia/reperfusion injury in striated muscle in hamsters. Proc Natl Acad Sci USA 1991, 88:6726–6730
26. Zeintl H, Sack FU, Intaglietta M, Messmer K: Computer assisted leukocyte adhesion measurement in intravital microscopy. Int J Microcirc Clin Exp 1989, 8:293–302
27. Menger MD, Pattenier A, Jäger S, Messmer K: Cryopreservation of islets of Langerhans does not affect angiogenesis and revascularization after free transplantation. Eur Surg Res 1992, 24:89–96
28. Lehr HA, Kröber M, Hübner C, Vajkoczy P, Menger MD, Nolte D, Kohlschütter A, Messmer K. Stimulation of leukocyte/endothelium interaction by oxidized low-density lipoprotein in hairless mice: involvement of CD11b/CD18 adhesion receptor complex. Lab Invest 1993, 68:388–395
29. Rutili G, Arfors KE: Technical report: fluorescein-labelled dextran measurement in interstitial fluid in studies of macromolecular permeability. Microvasc Res 1976, 12:59–70
30. Grant L: The sticking and emigration of white blood cells in inflammation. The Inflammatory Process. Edited by Grant L, Zweifach, BW, McCluskey, RT. New York, Academic Press, 1973, pp 205–249
31. Longnecker DE, Harris PD: Microcirculatory actions of general anesthetics. Fed Proc 1980, 39:1580–1583
32. Menger MD, Sack FU, Barker JH, Feifel G, Messmer K: Quantitative analysis of microcirculatory disorders after prolonged ischemia in skeletal muscle. Res Exp Med 1988, 188:151–165
33. Schmidt-Nielsen K, Pennycuik P: Capillary density in mammals in relation to body size and oxygen consumption. Am J Physiol 1961, 200:746–750
34. Ghose T, Ferrone S, Imai K, Norvell ST, Luner SJ, Martin RH, Blair AH: Imaging of human melanoma xenografts in nude mice with a radiolabeled monoclonal antibody. J Natl Cancer Inst 1982, 69:823–826